EXPERIMENTAL INVESTIGATION OF THE KINK EFFECT BY IMPACT TESTS ON POLYCARBONATE SHEETS

E. UHLMANN, M. POLTE, R. HÖRL, N. BERGSTRÖM, S. THOM, P. WITTWER

Institute for Machine Tools and Factory Management, Technische Universität Berlin, Pascalstraße 8 - 9, 10587 Berlin, Germany, E-mail: hoerl@iwf.tu-berlin.de

In machine tools, machine guard windows provide an insight into the working process of the machine and protect the user against possible ejection of parts during operation, such as chips, tools and workpiece fragments [1, 2]. To ensure the safety of the machine operator, impact tests can be used to determine or verify the impact resistance of the machine guard. Polycarbonate is the most commonly used material for machine guard windows due to its high toughness compared to other transparent materials. In general, an increase in sheet thickness results in an improved impact resistance. However, the studies of CORRAN ET AL. (1983) [3] show that for an increased sample thickness a reduction of the impact resistance occurs. The authors called this phenomenon Kink Effect. This contribution focusses on the investigation of the Kink Effect for monolithic polycarbonate sheets up to a thickness of 18 mm and a lathe standard projectile with a mass of 2.5 kg. Experiments were carried out to compare the material behavior of polycarbonate sheets under projectile impact for the dimensions of 300 mm (height) x 300 mm (width) and 500 mm (height) x 500 mm (width). The experiments were further evaluated using the RECHT & IPSON (1963) [4] method. Furthermore, explicit dynamic impact simulations were performed to enable the investigation of "close-to-edge" impacts.

Keywords: Impact test, Kink Effect, machine guard, safety of machinery.

1. Introduction

Standardized international regulations such as the standard ISO 23125 (2015) [1] regarding the safety of lathes offer a legal framework for the use of polycarbonate (PC) sheets in machine guard enclosures by providing a basis of design and specifying test procedures for an experimental verification of an adequate protection against ejected chips, tool or workpiece fragments. Current test procedures subject PC guard windows to a high-energy impact by a blunt projectile. The initial kinetic energy $E_{kin,i}$ of the projectile during the impact test, hereinafter referred to as initial projectile energy $E_{pr,i}$, dependents on the maximum foreseeable spindle speed n of the machine tool for which the guard window is used. The PC guard window is considered safe, in case of deforming without the formation of a through crack visible from one surface to the other, where the impacted side and the opposite side are referred to as machine side and operator side, respectively. Accordingly, the impact resistance Y is defined as the maximum initial projectile energy $E_{pr,i}$ a test sample withstands. For higher initial projectile energies $E_{pr,i}$ the test sample thickness d_{ts} of the PC guard window is usually increased in order to ensure sufficient safety [1]. CORRAN ET AL. (1983) [3] observed a partial reduction of the impact resistance Y, when increasing the test sample thickness d_{ts}, the so-called Kink Effect. This behavior represents a potential risk for the machine operator, since the design of safeguards is based on the assumption that a greater PC guard window thickness d leads to higher impact resistance Y. The projectile mass m_{pr}, nose shape and hardness have been shown to have a significant effect on penetration as does the target rigidity and support condition. The ductile materials structural steel, stainless steel and aluminum alloy studied by CORRAN ET AL. (1983) [3] showed a clear Kink Effect, associated with a change in energy absorption from pronounced plastic deformation to perforation with well-defined shear bands and no significant bulging. However, in the investigation of the material behavior for different test sample thicknesses d_{ts} projectiles for small arms weapons are considered, thus limiting the study to a projectile mass of $m_{pr} = 34.5$ g.

WITTNER [5] determined a nonlinear relation between impact resistance Y and the test sample thickness d_{ts} for a projectile mass of $m_{pr} = 0.1$ kg representing standard projectiles for impact tests on guards for milling machines according to ISO 16090-1 [6]. Though, only up to a test sample thickness of $d_{ts} = 12$ mm monolithic PC was used, while multi-layer test samples were partially used for a test sample thickness $d_{ts} > 12$ mm. For a test sample thickness $d_{ts} = 15$ mm a significant decrease in impact resistance Y was observed.

According to ISO 16090-1 [6] and ISO 23125 [1] the maximum kinetic energy E_{kin} of ejected parts in the event of damage on lathes exceeds the maximum kinetic energy E_{kin} of milling machines up to four times. Since the consideration of higher projectile energies E_{pr} represents a worst-case scenario for machine guard windows impact tests are carried out with a standard lathe projectile with a mass of $m_{pr} = 2.5$ kg. To study the impact resistance Y as a function of the test sample thickness d_{ts} monolithic PC

Proceedings of the 31th European Safety and Reliability Conference
Edited by Bruno Castanier, Marko Cepin, David Bigaud and Christophe Berenguer
 Published by Research Publishing, Singapore
ISBN: 981-973-0000-00-0 :: doi: 10.3850/981-973-0000-00-0 esrel2021-paper

sheets in a range of test sample thickness of 8 mm < d_{ts} < 18 mm are investigated.

Furthermore, a finite element (FE)-model is provided, which enables the investigation of further test sample dimensions for future studies. ROTH (2017) [7] investigated different material models regarding their suitability for impact simulations of PC sheets and found a hydrodynamic material model to be the most suitable one. STECCONI ET AL. (2020) [8] adopted the approach of ROTH (2017) [7] and conducted FE-simulations with three different types of projectiles, where the results of those simulations showed a good agreement with experimental findings. While both studies offer deep insight into the mechanics of impact tests, they did not investigate the impact resistance Y in relation to different test sample thicknesses d_{ts}.

A "close-to-edge" impact leads to a reduced deformation of the test sample and a significantly decrease of the impact resistance Y, which is also observed for increasing test sample thicknesses d_{ts}. For this reason, in the present work, FE-simulations are also used to relate the findings for different test sample dimensions to "close-to-edge" impacts next to the support frame. The simulations of "close-to-edge" impacts underline the potential risk of a decreasing impact resistance Y this phenomenon represents.

2. Kink Effect

For ductile materials, an effect occurs in which the impact resistance Y stagnates or even decreases for increasing test sample thicknesses $d_{ts.}$ An exemplary representation of the phenomenon for the minimal perforation Energy E_{pm} is shown in Fig. 1.

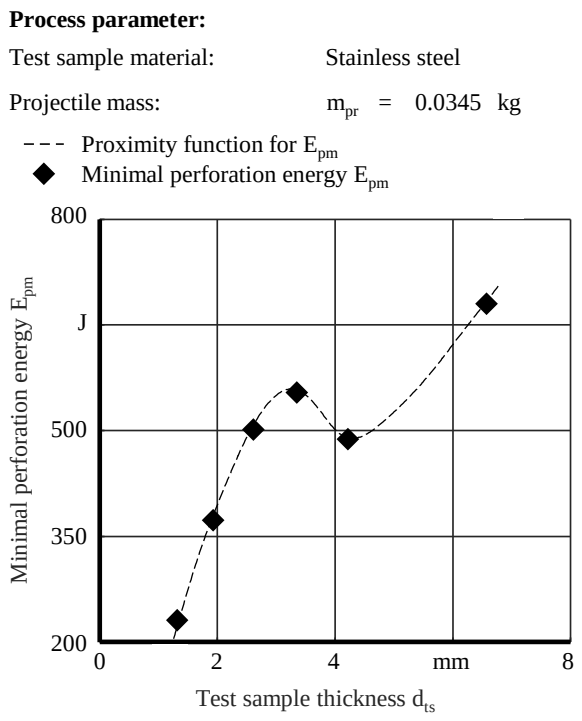

Fig. 1. Minimal perforation energy E_{pm} for different test sample thicknesses d_{ts} for the material stainless steel [3]

The minimal perforation energy E_{pm} and the associated minimal perforation velocity v_{pm} describe the case of a complete penetration of the test sample in which the projectile velocity v_{pr} after the penetration, the so-called residual projectile velocity $v_{pr,r}$, is $v_{pr,r}$ =0 m/s. This load-dependent behavior is called Kink Effect [3,5].

According to WITTNER [5], the Kink Effect can be explained by considering the energy balance of impact tests. Three mechanisms are of importance: elastic and plastic deformation as well as shear.

The energy input into the test sample depends solely on the initial projectile energy $E_{pr,i}$ of the projectile and is constant for a fixed projectile mass m_{pr} and initial projectile velocity $v_{pr,i}$. The sum of the aforementioned mechanisms is equal to the initial projectile energy $E_{pr,i}$ for $v_{pr,r} = 0$ or smaller than the initial projectile energy $E_{pr,i}$ for $v_{pr,r} > 0$. In case of an impact with minimal perforation velocity v_{pm} the energy balance can be described as shown in Eq. (1) [5].

$$E_{pr,i} = E_{pm} = E_e + E_p + E_s \tag{1}$$

However, the energy distribution varies with increasing test sample thickness d_{ts}. WITTNER [5] attributes the Kink Effect to a nonlinear exchange of energy among each other and derives the equation for each energetic term and their dependency on the test sample thickness d_{ts} and the bulging radius r_c of the PC sheet. Eq. (2) shows the energy of elastic deformation E_e, where σ_r is the yield stress and E the Young's modulus [3,5].

$$E_e = \frac{3\pi\, r_c^2\, d_{ts}\, (1 - v_{pr,i}^2)\, \sigma_r^2}{8\, E} \tag{2}$$

The elastic energy E_e depends linearly on the test sample thickness d_{ts} and quadratically on the bulging radius r_c.

The energy of plastic deformation is shown in Eq. (3), where r_p describes the projectile radius, N_0 the force of plastic membrane, ε_r the radial strain, M_0 the plastic yield moment, κ_r the radial curvature and κ_θ the circumferential curvature [3,5].

$$E_p = \int_{r_p}^{r_c} (N_0\, \varepsilon_r + M_0\, \kappa_r + M_0\, \kappa_\theta)\, 2\pi\, r\, dr \tag{3}$$

Solving the integral yields Eq. (4)

$$E_p = \frac{1}{2}\, C\, \left(r_c^2 - r_p^2\right) \tag{4}$$

with $C = (N_0\, \varepsilon_r + M_0\, \kappa_r + M_0\, \kappa_\theta)\, 2\pi$. The plastic energy E_p depends quadratically on the bulging radius r_c and is independent of the test sample thickness d_{ts}.

Eq. (5) represents the shear energy E_s. where e describes the shear area, τ_y the shear stress and γ_f the critical shear stress [3,5].

$$E_s = 2\pi \cdot r_p \cdot e \cdot d_{ts} \cdot \tau_y \cdot \gamma_f \tag{5}$$

The shear energy E_S depends linearly on the test sample thickness d_{ts} and is independent of the bulging radius r_c. For an increasing test sample thickness d_{ts} the bulging radius r_c decreases, thus resulting in a quadratic decrease of elastic and plastic deformation. The energy of both energetic terms is thereinafter transferred to shear resulting in material failure. Since the decrease of the bulging radius r_c is bounded by the projectile radius r_p the energy transfer from the elastic and plastic energetic term is bounded as well. For a further increase of the test sample thickness d_{ts} a point is reached where the shear energy E_s is dominant and leads to a linear increase of the minimal perforation energy E_{pm} for increasing test sample thicknesses d_{ts}.

3. Methods

3.1. *Experimental methods*

Fig. 2 shows the experimental setup used to determine the impact resistance Y of the test sample to be investigated. The initial projectile energy $E_{pr,i}$ is regulated by compressed air, built up in a pressure tank. The required initial projectile energy $E_{pr,i}$ can be affected by the variability of the acceleration pressure p_a and the acceleration length l_a inside the gun barrel.

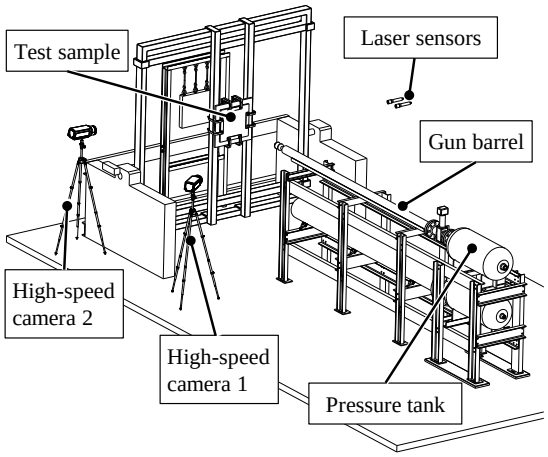

Fig. 2. Test facility at the INSTITUTE FOR MACHINE TOOLS AND FACTORY MANAGEMENT IWF OF TU BERLIN.

Projectile geometries, materials and masses m_{pr} are defined according to ISO 23125 (2015) [1] and shown in Fig. 3. The steel used for the projectile has the following mechanical properties:

- Tensile strength of 560 N/mm² ≤ R_m ≤ 690 N/mm²,
- Yield strength of $R_{p0.2}$ ≥ 330 N/mm² and
- Elongation rupture of A = 20 %.

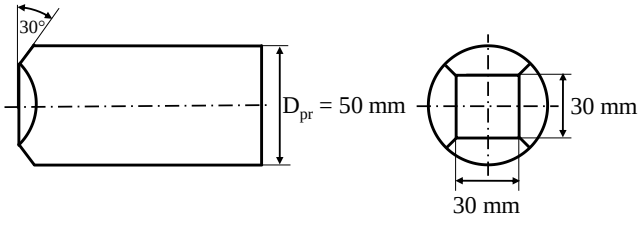

Fig. 3. Standardized projectile shape of a projectile with a mass of m_{pr} = 2.5 kg according to ISO 23125 (2015) [1].

Since the outer diameter D_{pr} of the projectile is smaller than the inner diameter of the gun barrel D_{gb}, the projectile is guided by two axially fixed polyamide plates. Before each test, radial notches are cut in the polyamide plates in order to break more easily when penetrating the test sample and thus minimizing the influence the impact tests.

The test sample is attached to a test sample frame with a contact width w_c = 25 mm, which in turn is attached to the test sample mount by screw clamps, as shown in Fig. 4. Fastening profiles are used to distribute the force applied by the screw clamps evenly over the PC test sample. The test samples are subjected to a central impact test according to ISO 23125 (2015) [1]. Square PC sheets with variable test sample thickness d_{ts}, test sample dimensions height h_{ts} and width w_{ts} are tested. A detailed description of the used test samples can be found in Table 4 (Appendix).

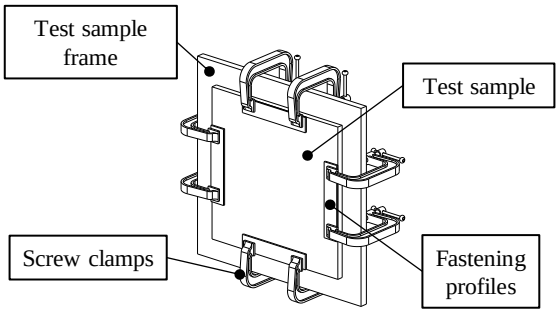

Fig. 4. Attachment of the test sample frame.

The different values of sample thickness d_{ts} represent commonly used values in the industry, whereas the test sample dimensions height h_{ts} and width w_{ts} are chosen based on ISO 23125 (2015) [1]. With 12 available test samples for each series, the following parameters were determined:

- impact resistance Y, which is the maximum initial projectile energy $E_{pr,i}$ a test sample withstands in order to pass an impact test,
- impact resistance velocity v_Y, which is the projectile velocity v_{pr} associated to the impact resistance Y,
- initial projectile velocity $v_{pr,i}$,
- residual projectile velocity $v_{pr,r}$, which is the velocity v_{pr} of the projectile after penetrating the test sample,
- minimal perforation velocity v_{pm}, which is the maximum initial projectile velocity $v_{pr,i}$ that results in a complete perforation of the test sample and a residual projectile velocity $v_{pr,r}$ = 0 m/s.

According to ISO 23125 (2015) [1], an impact test is passed, if the test sample deforms without the formation of a through crack visible from the machine side to the operator side.

Process parameter:
Test sample material: Polycarbonate - Arla MAKROCLEAR

Projectile mass:	m_{pr}	= 2.50	kg
Test sample heigth:	h_{ts}	= 300.00	mm
Test sample width:	w_{ts}	= 300.00	mm
Test sample thickness:	d_{ts}	= 12.00	mm

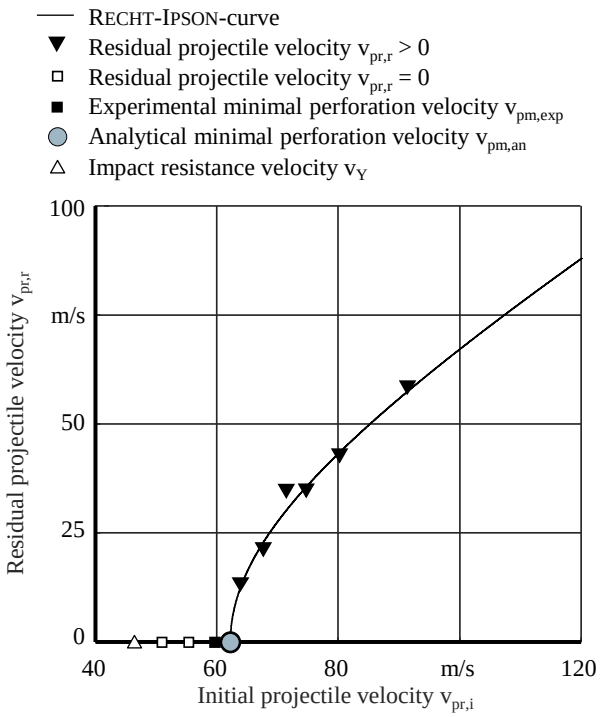

Fig. 5. Exemplary representation
of an impact test series and associated RECHT-IPSON-curve.

The impact resistance Y is generally determined by the bisection method and the minimal perforation velocity v_{pm} by the approach based on a study of RECHT & IPSON (1963) [4]. The minimal perforation velocity v_{pm}, however, does not exclude a failure of the test sample according to ISO 23125 (2015) [1]. The impact resistance velocity v_Y is less than the minimal perforation velocity v_{pm}. Although the impact resistance Y is of greater practical use, the minimal perforation velocity v_{pm} still is an important quantity, since it serves as an upper bound for the impact resistance Y and allows for a rough estimation of the impact resistance Y. The connection between the minimal perforation velocity v_{pm} and impact resistance Y is, however, still a subject of current research. For the bisection method a delimiting range of initial velocities $v_{pr,i}$ is defined, where the lower initial velocity $v_{pr,i,low}$ is below and the upper initial velocity $v_{pr,i,up}$ is greater than the impact resistance velocity v_y. Subsequently, additional impact tests are carried out to minimize the interval size. For a sufficient small interval, the impact resistance Y is directly derived from the tests. Although straightforward in design, the approach may lead to a large number of impact tests for an inappropriate chosen interval. Also, the bisection method may lead to incorrect results, since it does not account for statistical outliers.

RECHT & IPSON (1963) [4] provide an analytical approach to describe the residual velocity $v_{pr,r}$ of a projectile after penetrating a material as a function of its initial projectile velocity $v_{pr,i}$. LAMBERT & JONAS (1976) [9] recognized, that the RECHT-IPSON-equation, as a special case of a root function, requires a more advanced, generalized form by adding fitting parameters a and p. The relationship between the initial projectile velocity $v_{pr,i}$ and the residual projectile velocity $v_{pr,r}$ is shown in Eq. (6).

$$v_{pr,r} = \begin{cases} 0, & 0 < v_{pr,i} < v_{pm} \\ a \cdot \left(v_{pr,i}^{p} - v_{pm}^{p} \right)^{\frac{1}{p}}, & v_{pr,i} > v_{pm} \end{cases} \quad (6)$$

The fitting parameters a and p introduced by LAMBERT & JONAS (1976) [9] allow for the approximation of the function defined by Eq. (6) by means of the least-square-method. In the following curves based on Eq. (6) will be referred to as RECHT-IPSON-curve. Fig. 5 shows an example of the results of an impact test and the RECHT-IPSON-curve for PC test samples with a test sample height h_{ts} = 300 mm, a test sample width w_{ts} = 300 mm and a test sample thickness d_{ts} = 12 mm.

3.2 Numerical methods

The experimental investigations are accompanied by finite element simulations using the explicit solver of the commercial FE-software ANSYS MECHANICAL 2020, CANONSBURG, USA. Fig. 6 shows the model used for the explicit dynamic impact simulation.

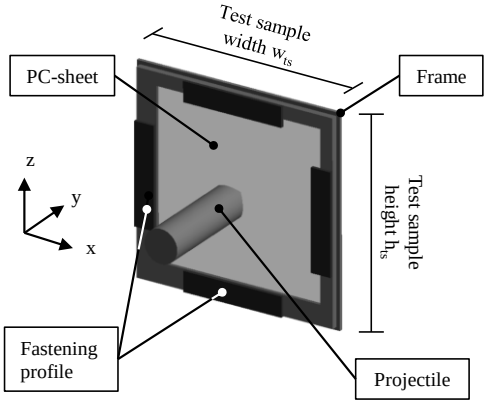

Fig. 6. Schematic representation of the FE-model.

Frame and projectile are modeled as elastic parts with the material properties of mild steel, i. e. a Young's modulus E = 200 GPa, a density of ρ = 7,850 kg/m^3 and a Poisson's number ϑ = 0.3. The fastening profiles make use of an elastic material formulation modelling hardwood with a Young's modulus of E = 11.3 GPa, a density ρ = 607 kg/m^3 and a Poisson's number ϑ = 0.37. Tetrahedron elements were used for the meshing of the PC sheets, with a finer mesh at the impact point and a coarser mesh towards the frame. The average minimum element size $l_{FE,min}$ at the impact point was set to $l_{FE,min}$ = 1.5 mm. Due to the fixed minimum element size $l_{FE,min}$ the number of elements in the y-direction of the PC sheets increases with the test sample thickness d_{ts}. A detailed description of the mesh parameters used in the FE-simulations can be found in Table 6 in the appendix. To properly describe the behavior of the PC sheets the approach of STECCONI ET AL. [8] is adopted, which uses a hydrodynamic material model based on the

MIE-GRUNEISEN equation of state in conjunction with a multilinear hardening curve. This material model allows to calculate the pressure as shown in STECCONI ET AL. [8] and is based on a set of parameters describing the shock wave propagation velocity U. The parameters for the MIE-GRUNEISEN equation of state are taken from the material database of ANSYS 2020. Parameters of the hardening curve are taken from a study of WALLEY ET AL. [10]. The outside facing surfaces of the frame and strips are fixed both translationally and rotationally by boundary conditions, whereas an initial velocity $v_{pr,i}$ in y-direction is applied to the projectile. Similar to the experiment the simulations adopt the RECHT-IPSON-method to derive to minimal perforation velocity v_{pm} of the PC-sheets. For that, different initial velocities $v_{pr,i}$ are applied to the projectile. The experimental results are used to validate the FE-model.

4. Results and discussion

Fig. 7 shows exemplary the experimental results with a test sample width of w_{ts} = 500 mm, height of h_{ts} = 500 mm and thickness of d_{ts} = 12 mm. The corresponding RECHT-IPSON-curve was calculated using test results with a residual projectile velocity $v_{pr,r}$ > 0 m/s. Impact tests which lead to a residual projectile velocity $v_{pr,r}$ = 0 m/s can be found on the x-axis. In those cases, the test sample was only partially penetrated or plastically deformed.

Process parameter:

Test sample material: Polycarbonate - Arla MAKROCLEAR

Projectile mass:	m_{pr}	=	2.50 kg
Test sample heigth:	h_{ts}	=	500.00 mm
Test sample width:	w_{ts}	=	500.00 mm
Test sample thickness:	d_{ts}	=	12.00 mm

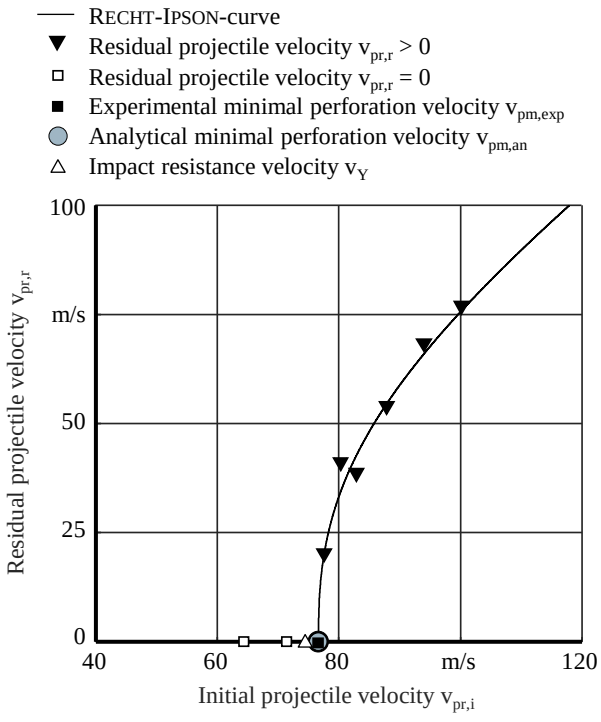

Fig. 7. Experimental results of the impact test and derived RECHT-IPSON-curve for test sample dimension w_{ts} = h_{ts} = 500 mm

The intersection of the RECHT-IPSON-curve with the x-axis represents the analytically determined minimal perforation velocity $v_{pm,an}$. The used fitting parameters for the RECHT-IPSON-curves and the corresponding analytical minimal perforations velocities $v_{pm,an}$ can be found in Table 5 in the appendix.

Fig. 8 and Table 4 in the appendix show the experimentally derived impact resistance velocity v_Y as a function of test sample thickness d_{ts} for test samples with a width w_{ts} = 300 mm and a height h_{ts} = 300 mm and test samples with a width of w_{ts} = 500 mm and a height of h_{ts} = 500 mm. The graph in Fig. 8 clearly shows the significant influence of width w_{ts} and height h_{ts} on the impact resistance velocity v_Y of the test samples. For the same thickness d_{ts} the impact resistance velocity v_Y differs by 34 % for a test sample thickness of d_{ts} = 8 mm and increases up to 53 % for a test sample thickness of d_{ts} = 18 mm. A possible explanation for the difference is the deformation behavior of the PC sheets. Smaller PC sheets of width w_{ts} = 300 mm and a height h_{ts} = 300 mm present a more local deformation behavior compared to PC sheets of width w_{ts} = 500 mm a height h_{ts} = 500 mm. A more localized deformation leads to less global bulging of the test sample and an energy concentration around impact point, thus causing the test sample to fail and resulting in a generally lower impact resistance velocities v_Y than test samples of width w_{ts} = 500 mm and height h_{ts} = 500 mm. Furthermore, a general trend towards higher impact resistance velocities v_Y can be observed when the test sample d_{ts} is increased.

Process parameter:

Test sample material: Polycarbonate - Arla MAKROCLEAR

Projectile mass: m_{pr} = 2.50 kg

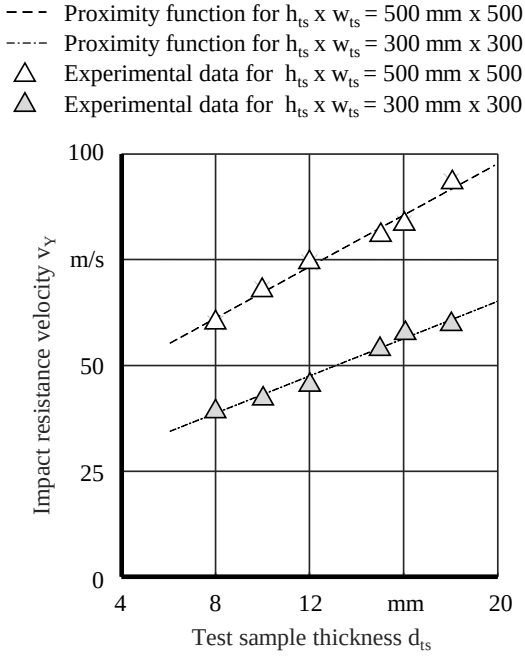

Fig. 8. Impact resistance velocity v_Y as a function of the test sample thickness d_{ts} for experimental results

In contrast to WITTNER [5] no pronounced stagnation or even decrease of the impact resistance Y or the associated impact resistance velocity v_Y respectively could be found. A continuous linear increase of the impact resistance velocity v_Y with increasing test sample thickness d_{ts} can be observed for both test sample dimensions considered, indicated by the proximity function. The experimental data was approximated using a linear approach with the corresponding squared norm residual as measure for accuracy of the approach shown in Table 1.

Table 1. Error of the proximity function for the impact resistance velocity v_Y.

Sample dimensions h_{ts} x w_{ts} (mm x mm)	300 x 300	500 x 500
Squared norm residual (m^2/s^2)	2,71	4,07

However, it should be noted that WITTNER [5] conducted impact tests according to ISO 16090-1 [6] and thus used a smaller projectile with a mass of m_{pr} = 0.1 kg. The smaller projectile mass m_{pr} causes a different mechanical response of the PC sheet to the impact and a different energy distribution and thus the occurrence of a pronounced Kink Effect. Hence, it is suggested that the Kink effect occurs at smaller test sample thicknesses of d_{ts} < 8 mm or greater test sample dimensions in impact tests according to ISO 23125 [1] with a projectile mass of m_{pr} = 2.5 kg.

Fig. 9 and Fig. 10 show a comparison of the analytical minimal perforation velocity $v_{pm,an}$ calculated via least-square-method using Eq. (6), the minimal perforation velocity $v_{pm,exp}$ obtained from experimental impact tests and the numerical minimal perforation velocity $v_{pm,num}$ determined by FE-simulations. Table 7 in appendix presents the associated data. Experimental and analytic data show good agreement for both cases confirming the accuracy of the analytical approach, where a better agreement can be seen for a test sample dimensions of $w_{ts} = h_{ts}$ =500 mm. For test sample dimensions $w_{ts} = h_{ts}$ =300 mm the deviation between experimental and numerical results tends to decrease towards a higher test sample thickness d_{ts}, starting with a deviation of 32 % for a test sample thickness of d_{ts} = 8 mm decreasing to 7 % for a test sample thickness of d_{ts} = 16 mm.

A similar deviation between experiment and simulation can be observed for test sample dimensions $w_{ts} = h_{ts}$ =500 mm, where the largest deviation of 17 % occurs for a test sample thickness of d_{ts} = 8 mm decreasing constantly to 6 % for a test sample thickness of d_{ts} = 18 mm. The discrepancy between experimental and numerical results indicate inadequacies in the material model used for the FE-simulations.

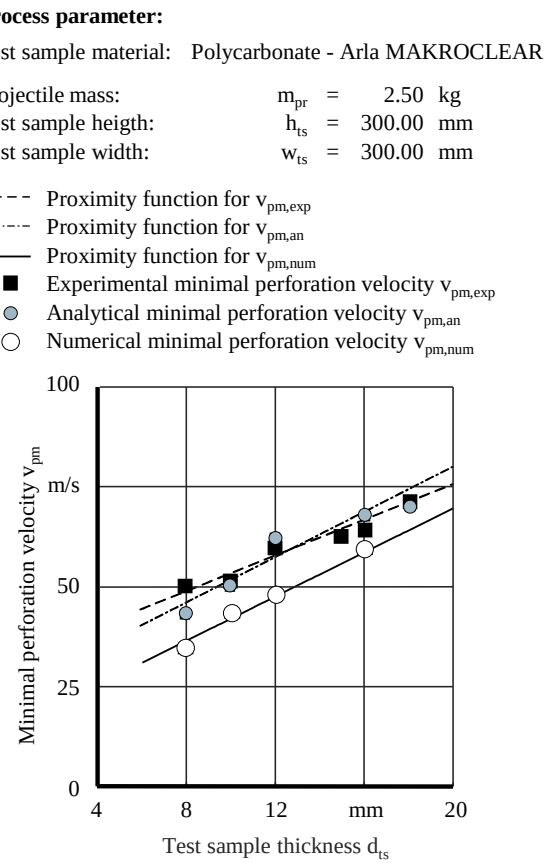

Fig. 9. Comparison of results for the minimal perforation velocity v_{pm}, test sample dimensions of $w_{ts} = h_{ts}$ = 300 mm.

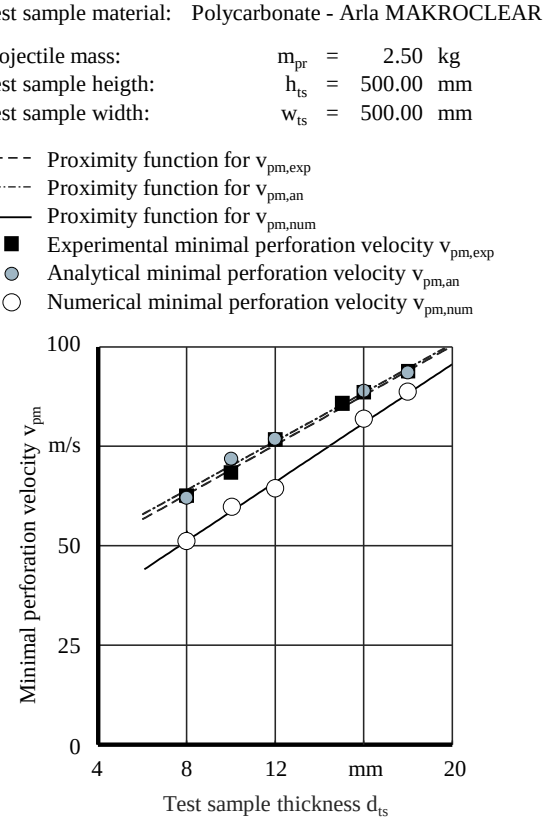

Fig. 10. Comparison of results for the minimal perforation velocity v_{pm}, test sample dimensions of $w_{ts} = h_{ts}$ = 500 mm.

Nonetheless, the FE-simulations allow for an investigation of the influence of the bulging radius r_c by relating the mechanisms causing the Kink Effect to the test sample dimensions and "close-to-edge" impacts next to the support frame. In a first approximation, impact tests for a test sample width of w_{ts} = 300 mm and height of h_{ts} = 300 mm can be considered as “close-to-edge” impacts for a test sample width of w_{ts} =500 mm and a height of h_{ts} = 500 mm, as shown in Fig. 11.

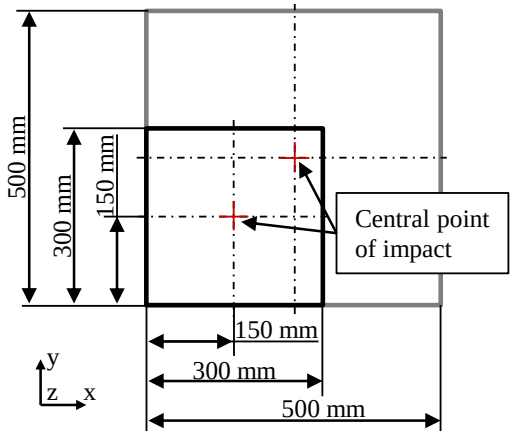

Fig. 11. Schematic representation of the relationship between different test pattern dimensions and “close-to-edge” impacts.

For the study of “close-to-edge” impacts, three cases are considered shown in Fig. 12:

- Case 1: central impact, test sample dimensions of w_{ts} = h_{ts} = 300 mm, test sample thickness d_{ts} = 16 mm,
- Case 2: central impact, test sample dimensions of w_{ts} = h_{ts} = 500 mm, test sample thickness d_{ts} = 16 mm,
- Case 3: “close-to-edge” impact with an offset of $dist_{off}$ = 100 mm in z-direction and x-direction, test sample dimensions of w_{ts} = h_{ts} = 500 mm, test sample thickness of d_{ts} = 16 mm.

In all three cases the test sample is subjected to the same impact velocity $v_{pr,i}$ = 80 m/s. Fig. 12 and Table 2 show the maximum deformation y_{max} in y-direction and the bulging radius r_c of the test sample due to the impact of the projectile for the different cases. A clear difference of bulging radius r_c can be observed for each simulation, where case 2 shows the greatest bulging radius r_c.

The results of the simulations match the predictions made by WITTNER [5], where according to Eq. (1) a greater bulging radius r_c leads to a larger proportion of elastic deformation resulting in a larger maximum deformation y_{max}.

Table 2. Comparison of maximum test sample displacement y_{max} and bulging radius r_c

Case	Sample dimensions w_{ts} x h_{ts}	Projectile velocity $v_{pr,r}$	Maximum displacement y_{max}	Bulging radius r_c
	(mm x mm)	(m/s)	(mm)	(J)
1	300 x 300	44	48	105
2	500 x 500	0	70	195
3	500 x 500	39	56	160

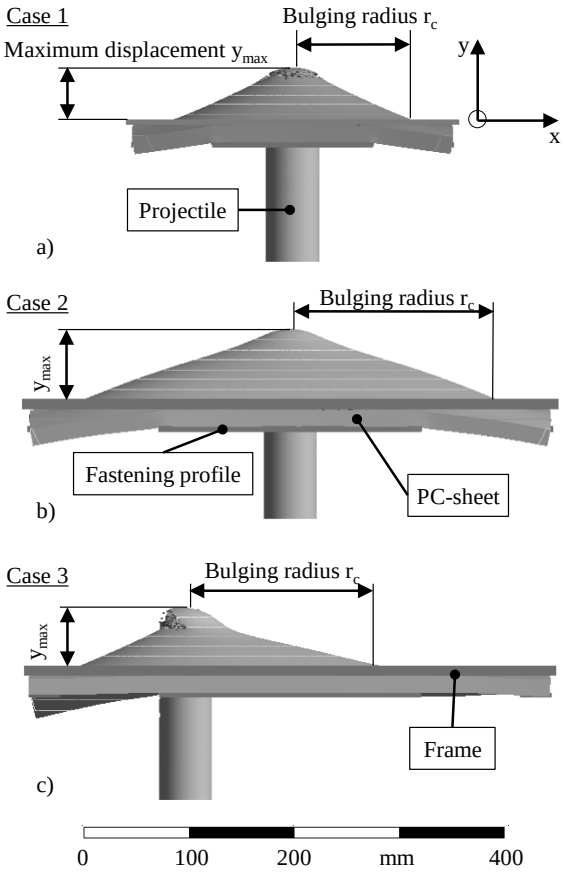

Fig. 12. Comparison of different impact test cases;
a) Central impact, test sample dimensions w_{ts} = h_{ts} = 300 mm;
b) Central impact, test sample dimensions w_{ts} = h_{ts} = 500 mm;
c) “close-to-edge” impact, test sample dimensions w_{ts} = h_{ts} = 500 mm

Though in Case 3 the identical test sample dimension w_{ts} = h_{ts} = 500 mm were subjected to the identical impact load like Case 2 it shows fewer elastic deformation and hence a greater proportion of shear resulting in material failure and a residual projectile velocity $v_{pr,r}$ > 0 m/s. A similar behavior can be observed for Case 1, where due to the smaller test sample dimension of w_{ts} = h_{ts} = 300 mm a smaller bulging radius r_c leads fewer elastic deformation and a greater proportion of shear and material failure. Since in Case 1 the bulging radius r_c is smaller than the bulging radius r_c of Case 3 material failure occurs at an earlier stage resulting in a greater residual projectile velocity $v_{pr,r}$ than in Case 3.

The possibility of connecting “close-to-edge” impacts for test samples with a width w_{ts} = 500 mm and a height h_{ts} = 500 mm to impacts of width w_{ts} =300 mm and heigth h_{ts} = 300 mm with a central point of impact allows a critical discussion of the permissible thickness d of safe guards specified in ISO 23125 [1]. Table 3 shows a comparison of the maximum initial projectile energy $E_{pr,i}$ permitted according to ISO 23125 [1] for different thicknesses d. Furthermore, the experimental results for test sample dimensions width w_{th} = 300 mm and height h_{ts} = 300 mm are shown. The impact resistance Y was derived from the results of the impact resistance velocity v_Y in Table 4, using the projectile mass of m_{pr} = 2.5 kg.

Table 3. Comparison of the impact resistance Y according to ISO 23125 [1] and the experimental results for test sample dimensions width w_{ts} = 300 mm and height h_{ts} = 300 mm.

Test sample thickness d_{ts}	Impact resistance Y according to ISO 23125 [1].	Impact resistance Y for test sample dimensions width w_{ts} =300 mm, height h_{ts} =300 mm
(mm)	(J)	(J)
8	3,124	1,982
10	4,960	2,021
12	4,960	2,640
16	4,960*	4,224
18	-	4,543
19	8,000	-

The value marked with an asterisk for a test sample thickness of d_{ts} = 16 mm were determined using a compound of two PC sheets with a test sample thickness of d_{ts} = 8 mm, which might affect the results and thus does not allow for a direct comparison. However, the impact resistance Y for test sample dimensions of width w_{ts} = 300 mm and height h_{ts} = 300 mm fall below the values defined in ISO 23125 [1] for every safe guard thickness d. Though being only an estimate for the impact resistance of PC sheets with a width w_{ts} = 500 mm and a height h_{ts} = 500 mm for "close-to-edge" impacts the results imply that a central impact test might overestimate the impact resistance Y for PC sheets significantly. The potential risk of eccentric impacts shown by these results might be neglected completely by today's safety standards.

5. Conclusion & outlook

In this investigation, the impact resistance Y and minimal perforation velocity v_{pm} were determined by experimental impact tests using standard lathe projectile with a mass of m_{pr} = 2.5 kg. For the evaluation of the test series, the approach of LAMBERT & JONAS (1976) [9] was applied, which uses the RECHT & IPSON (1963) [4] method. The focus was placed on the influence of the test sample thickness d_{ts} on the impact resistance Y behavior. Experimental impact tests on PC sheets were conducted with a test sample width w_{ts} = 300 mm and test sample height h_{ts} = 300 mm, test sample width w_{ts} =500 mm and test sample height h_{ts} = 500 mm and test sample thicknesses of 8 mm ≤ d_{ts} ≤ 18 mm. The results of the analytically derived minimal perforation velocity $v_{pm,an}$ are in good agreement with the experimental results.

A linear increase of the impact resistance velocity v_Y with increasing test sample thickness d_{ts} was found for the test sample dimensions with test sample width w_{ts} = 500 mm and height h_{ts} = 500 mm and also for test sample width of w_{ts} = 300 mm and height of h_{ts} = 300 mm. This leads to the conclusion that no Kink Effect is present for the investigated parameters. A possible explanation is that the Kink Effect occurred in a test sample thickness range of d_{ts} < 8 mm. Thus, no plastic deformation Energy E_p but mainly shear energy E_S was present during the impact tests for the investigated parameter range. For projectiles such as standard projectiles with a mass of m_{pr} = 0.625 kg and a smaller impact area or increased test sample dimensions such as width w_{ts} =800 mm and height h_{ts} = 800 mm a Kink Effect could occur in the range of the investigated test sample thicknesses d_{ts} due to possible higher amount of plastic deformation energy E_p in the investigated parameter range.

Furthermore, a clear difference in impact resistance Y was found for the two investigated test sample dimensions w_{ts} and h_{ts}. The values for test samples with a width w_{ts} =300 mm and height h_{ts} = 300 mm were significantly lower than the values of test samples with a width w_{ts} =500 mm and height h_{ts} = 500 mm for all test sample thicknesses d_{ts}. This shows that a reduction of the area for deformation on the test sample, as in the case of "close-to-edge" impacts, leads to a significant reduction of the impact resistance Y.

The FE-model used in this work was not capable to adequately represent the experimentally determined minimal perforation velocity v_{pm}. Future work aims to reduce the discrepancies between experimental and numerical results by improving the FE-material model and subsequently conduct investigations for further test sample dimensions such as tests sample with a width of w_{ts} = 800 mm and height of h_{ts} = 800 mm.

The findings can be used for the design of PC guard windows and to predict their behavior in the case of projectile impact to ensure the safety of machine operators. Additionally, the results provide insight into the material behavior in the case of "close-to-edge" impact.

References

1. DIN EN ISO 23125, Machine tools safety -turning machines, (2015).
2. DGUV Deutsche Gesetzliche Unfallversicherung, Schutzscheiben an Werkzeugmaschinen der Metallverarbeitung, DUGV-Information FB HM-040, (2018).
3. R.S.J. Corran, P.J. Shadbolt, C. Ruiz, Impact loading of plates - An experimental investigation, International journal of impact engineering 1, (1983).
4. R.F. Recht, T.W. Ipson, Ballistic perforation dynamics, Journal of applied mechanics, 384 – 390, (1963).
5. Wittner, M.: Leichtbau im Maschinenschutz - Umsetzungs-strategien und Konzepte. Berlin, Technische Universität Berlin, Dissertation. Institut für Werkzeugmaschinen und Fabrikbetrieb, (2008).
6. DIN EN ISO 16090-1, Machine tools safety - machining centres, milling machines, transfer machines
7. M. Roth, Hybrid structures under ballistic loading, Springer Vieweg, (2017).
8. A. Stecconi, L. Landi, Finite element analysis for impact tests on polycarbonate safety guards: Comparison with experimental data and statistical dispersion of ballistic Limit, Journal of Risk and Uncertainty in Engineering Systems, Part B: Mechanical Engineering, (2020).
9. J.P. Lambert, G.H. Jonas, Towards standardization in terminal ballistics testing, (1976).
10. S.M- Walley, J.E. Field, Strain Rate Sensitivity of Polymers in Compression from Low to High Rates, Dymat Journal, 221 – 227, (1994).

Appendix

Table 4. Overview of test series and results for the impact resistance Y.

Test series	Test sample thickness d_{ts}	Test sample dimensions w_{ts} x h_{ts}	Impact resistance velocity v_Y
	(mm)	(mm x mm)	(m/s)
1	8	300 x 300	39.82
2	10	300 x 300	42.59
3	12	300 x 300	45.96
4	15	300 x 300	54.30
5	16	300 x 300	58.13
6	18	300 x 300	60.29
7	8	500 x 500	60.39
8	10	500 x 500	68.42
9	12	500 x 500	74.58
10	15	500 x 500	80.13
11	16	500 x 500	83.98
12	18	500 x 500	93.89

Table 5. Fitting parameters of the RECHT-IPSON-curves and results of the the analytical minimal perforation velocity $v_{pm,an}$.

Test series	Fitting parameter a	Fitting parameter p	Analytical minimal perforation velocity $v_{pm,an}$	Squared norm of residual
	(-)	(-)	(m/s)	(m^2/s^2)
1	1.00	1.44	43.74	63.00
2	1.00	1.51	50.55	51.86
3	0.83	2.11	62.86	20.94
4	0.50	3.64	71.96	0.78
5	1.00	1.40	67.88	27.40
6	0.98	1.42	70.21	1.39
7	1.00	2.57	62.19	25.19
8	0.87	3.85	71.62	27.10
9	0.99	2.60	76.62	63.62
10	1.00	2.35	87.78	0.01
11	0.71	4.41	89.13	35.66
12	1.00	2.45	93.55	6.18

Table 6. Mesh parameters used for the FE-simulations.

Test series	Number of elements	Number of nodes	Average minimum element size $l_{FE,min}$
	(-)	(-)	(mm)
1	345,586	71,766	1.5
2	419,735	83,981	1.5
3	503,226	98,177	1.5
4	-	-	-
5	647,978	122,805	1.5
6	732,892	137,079	1.5
7	400,264	84,075	1.5
8	491,829	99,395	1.5
9	577,180	113,778	1.5
10	-	-	-
11	736,536	140,307	1.5
12	815,465	153,457	1.5

Table 7. Comparison of the experimental minimal perforation velocity $v_{pm,exp}$, the analytical minimal perforation velocity $v_{om,an}$ and the numerical minimal perforation velocity $v_{pm,num}$.

Test series	Experimental minimal perforation velocity $v_{pm,exp}$	Analytical minimal perforation velocity $v_{pm,an}$	Numerical minimal perforation velocity $v_{pm,num}$
	(m/s)	(m/s)	(m/s)
1	50.66	43.74	33.51
2	51.28	50.55	39.59
3	60.08	62.86	46.11
4	62.47	71.96	-
5	64.48	67.88	55.69
6	74.46	70.21	-
7	62.61	62.19	51.96
8	68.42	71.62	59.86
9	76.75	76.62	64.93
10	85.52	87.78	-
11	88.63	89.13	81.78
12	93.89	93.55	88.79